J Therm Anal Calorim (2014) 117:693–699
DOI 10.1007/s10973-014-3833-0

Synergistic effect of organophilic Fe-montmorillonite on flammability in polypropylene/intumescent flame retardant system

Hong Liu · Qi Zhong · Qinghong Kong · Xingguang Zhang · Yanjun Li · Junhao Zhang

Received: 6 November 2013 / Accepted: 22 April 2014 / Published online: 10 May 2014

Abstract Polypropylene/intumescent flame retardant/organophilic Fe-montmorillonite (PP/IFR/Fe-OMT) nanocomposites were prepared by melting intercalation. In order to investigate the effect of structural Fe^{3+} in the PP/IFR system, the corresponding PP/IFR and PP/IFR/Na-OMT composites were prepared under the same conditions. The thermo-gravimetric analysis data show that the PP/IFR/Fe-OMT nanocomposites have higher thermal stability than the PP/IFR and PP/IFR/Na-OMT composites. The flame retardant results indicate that the limiting oxygen index values of the nanocomposites with Fe-OMT are basically higher than those of the pure PP and the composites containing IFR or Na-OMT/IFR. And the addition of a suitable amount of Fe-OMT in PP/IFR composites can apparently favor UL94 test, and no dripping phenomenon was found. The cone calorimeter test indicates that the heat release rate (HRR) is significantly reduced by the formation of the nanocomposites, and the HRR of the PP/IFR/Fe-OMT nanocomposites are decreased in comparison with those of the PP/IFR/Na-OMT nanocomposites. It is noteworthy that Fe-OMT is helpful to smoke suppression by smoke density test.

Keywords Polypropylene · Intumescent flame retardant · Nanocomposite · Heat release rate · TG

H. Liu · Q. Zhong · Q. Kong (✉) · X. Zhang · Y. Li
School of the Environment and Safety Engineering, Jiangsu University, Zhenjiang 212013, Jiangsu, China
e-mail: kongqh@ujs.edu.cn; kongqh@mail.ujs.edu.cn

J. Zhang (✉)
School of Biological and Chemical Engineering, Jiangsu University of Science and Technology, Zhenjiang 212018, Jiangsu, China
e-mail: jhzhang6@mail.ustc.edu.cn

Introduction

Polypropylene (PP) is widely used in apparel, floor coverings, hygiene medical, geotextiles, car industry, automotive textiles, various home textiles, wall-coverings, and so on [1–3]. However, the inherent flammability of PP, with a limiting oxygen index (LOI) typically of 17, limits its application in some fields like electronic appliances where high flame retardancy is required. To reduce flammability, the addition of flame retardants is an effective way. Moreover, the use of intumescent flame retardant (IFR) in polyolefins is a relatively recent technology as compared to the development and extensive use of the polyolefins themselves [4–6]. It is well known that the IFR is known as a new generation of flame retardants for polyolefins (such as polyethylene and PP) due to its advantages, such as low-smoke, low release of toxic gasses during burning, and antidripping [7, 8].

However, it also has some drawbacks as compared to halogen-containing flame retardants [9, 10]. For instance, low flame-retardant efficiency and IFR needs more additive amount to achieve the results obtained with the halogenated compound. To reduce the amount of IFR in polymer composites, some synergistic agents, such as clay [11], some transition metal oxides, and metal compounds [12–16], have been used as synergistic agent, which can improve flame-retardant effect and thermal stability of char residues through catalytic reactions among the components of the IFR system [17, 18]. In our study, inspired by the effectiveness of iron and montmorillonite, Fe-montmorillonite (Fe-MMT) was prepared and used as synergistic agent to improve the flame retardancy in PP/IFR composites. The Fe-MMT has the same crystal structure and the Fe^{3+} ion replaces Al^{3+} ion in the crystal lattice comparing to Na-MMT. Fe-MMT is modified by

cetyltrimethyl ammonium bromide (CTAB) to obtain organic modification Fe-MMT (Fe-OMT). In order to discuss the effect of iron in the PP/IFR system, the corresponding PP/IFR/Na-OMT nanocomposites were prepared under the same conditions. Thermal properties and flame retardancy were investigated using TG, LOI, UL-94 vertical burning test, cone calorimeter test (CCT), and smoke density test (SDT).

Experimental

Materials

Polypropylene (PP, F401), maleic anhydride grafted PP (PP-g-MA), IFR, Na-montmorillonite (Na-MMT), Fe-MMT (synthesized as follows: hydrous oxide was prepared by mixing $Na_2SiO_3 \cdot 9H_2O$ with $FeCl_3 \cdot 6H_2O$ and $Zn(CO\text{-}OCH_3)_2 \cdot 2H_2O$ solutions to set the atomic ratio at Si–Fe–Zn = 4–1.7–0.3; the detailed method of synthesis followed previous reports [19]). The Na-MMT and Fe-MMT were modified by CTAB, and the products were labeled as Na-OMT and Fe-OMT, respectively.

Preparation of the nanocomposites

The PP (the content of PP-g-MA was 10 % in PP matrix), additives, and desired amounts of Na-OMT, Fe-OMT, and IFR were premixed, then extruded at 180 °C using an internal mixer (SU-70, Jiangsu, China) at 60 rpm for 10 min. Afterward, the nanocomposites were compression molded into sheets of 1 mm by a hot press at 180 °C and 10 MPa for 10 min, followed by cooling to room temperature. All of the details about the samples are listed in the Table 1.

Table 1 The composition of the samples

samples	PP/%	IFR*/%	Fe-OMT/%
PP0	100		
PP1	80	20	
PP2	80	16	4
PP3	76	24	
PP4	76	22	2
PP5	76	20	4
PP6	76	18	6
PP7	76	20	4 (Na-OMT)
PP8	72	28	
PP9	72	24	4

* IFR = 45 %APP + 20 %PER + 35 %MPP

Characterization

X-ray diffraction (XRD) was used to characterize the layer conformation of the nanocomposites. The operating parameters were Cu Kα ($\lambda = 1.54178$ Å) radiation at a generator voltage of 40 kV and current of 100 mA. The range of the diffraction angle was $2\theta = 1.5$–10°.

Transmission electron microscopy (TEM) specimens were cut at room temperature using an ultramicrotome (Ultracut-1, UK) with a diamond knife from an epoxy block containing the embedded films of the formulations. TEM images were obtained by JEOL JEM-100SX at an accelerating voltage of 100 kV.

The thermo-gravimetric analysis (TG) of PP nanocomposites was investigated by a TA50 Thermoanalyzer instrument. In each case, about 10 mg specimens were heated from 40 to 600 °C at the rate of 10 °C min^{-1} under an N_2 flow.

LOI was measured according to ASTM D2863. The apparatus used was an HC-2 oxygen index meter (Jiangning Analysis Instrument Company, China). The specimens used for the test were of dimensions $100 \times 6.5 \times 3.0$ mm^3. The result was averaged from 15 specimen tests in the LOI.

According to the UL-94 test, the sample rod ($130 \times 12.7 \times 3.0$ mm) was placed in a holder in a vertical position and the lower end of the rod contacted with a flame for 10 s to initiate burning. The second ignition was made after self-extinguishment of the flame at the sample. The burning process was characterized by the times t_1 and t_2 pertaining to the two burning steps. The parameters t_1 and t_2 denote the time between removing the methane flame and self-extinguishment of the sample. Moreover, it is always noted whether drips from the sample were released or drips made absorbent cotton flame during the burning times t_1 and t_2. The result was averaged from five specimen tests in the UL94.

The SDT evaluations of the samples, in the form of plates measuring $25.3 \times 25.3 \times 3$ mm^3, were done in accordance with ASTM E 662 by means of a General Model JCY-1 instrument (Jiangning Analysis Instrument Factory). The method is to measure the light absorption rate of the smoke during the initial period of the 4-min period of burning time. A special smoke chamber made of heat insulated material, ($300 \times 300 \times 750$ mm^3) ± 5 mm^3 in internal size, was used. The chamber was equipped with an ignition system, an illuminance measuring system, and a ventilation system. The result was averaged from five specimen tests in the SDT.

The signals from the cone calorimeter were recorded and analyzed by a computer system. All samples ($100 \times 100 \times 3.0$ mm^3) were examined in a Stanton Redcroft cone calorimeter according to ASTM 1356-90 under a heat flux of 50 kW m^{-2}. The experiments were

repeated three times and the results were reproducible to within ±10 %. The cone data reported in this paper are the average of three replicated experiments.

Results and discussion

The structure of PP/IFR/Fe-OMT composites

XRD was employed to characterize the layer conformation of nanocomposites. The *d*-spacing of Fe-OMT was 2.8 nm and the Na-OMT was 2.4 nm in our previous report [19]. Figure 1 showed XRD patterns of PP/IFR/Fe-OMT and PP/IFR/Na-OMT composites, in which the different states of the two types of nanocomposites can be found. The PP/IFR/Fe-OMT nanocomposites had no obvious diffraction peak at low content of clay (shown in Fig. 1a, b), which indicated that the nanocomposites were exfoliated or disordered structures. In contrast to PP/IFR/Fe-OMT nanocomposites, the PP/IFR/Na-OMT (4 % clay) nanocomposites had weak diffraction peaks in Fig. 1d, indicating that intercalated nanocomposites were obtained. The difference between PP/IFR/Fe-OMT and PP/IFR/Na-OMT nanocomposites was probably caused by the different *d*-spacing of the modified clay. When the content of Fe-OMT was increased to 6 %, a clear diffraction peak appeared in Fig. 1c. The appearance of the secondary and tertiary diffraction peaks declared the existence of intercalated nanocomposites. The result illustrates that the structures can be changed via the Fe-OMT content.

Figure 2 showed TEM images of the PP/IFR/Fe-OMT nanocomposites. The bright region represents the polymer matrix and the dark stripes represent the particles of IFR (A) and Fe-OMT (B). From Fig. 2b and c, it can be observed that the clay (4 % for both Fe-OMT and Na-OMT) was dispersed uniformly in the matrix. TEM images of PP4 and PP6 (2 and 6 % Fe-OMT, respectively) were shown in Fig. 2a and d; Fe-OMT layers are dispersed uniformly and irregularly in the PP matrix when the content of Fe-OMT is 2 %. However, when the content of Fe-OMT is 6 %, the nanocomposites have intercalated and exfoliated structures in Fig. 2d. When the Fe-OMT content increased, the dispersion was descended and the structure of nanocomposites were exfoliated to intercalated, consistent with the XRD analysis.

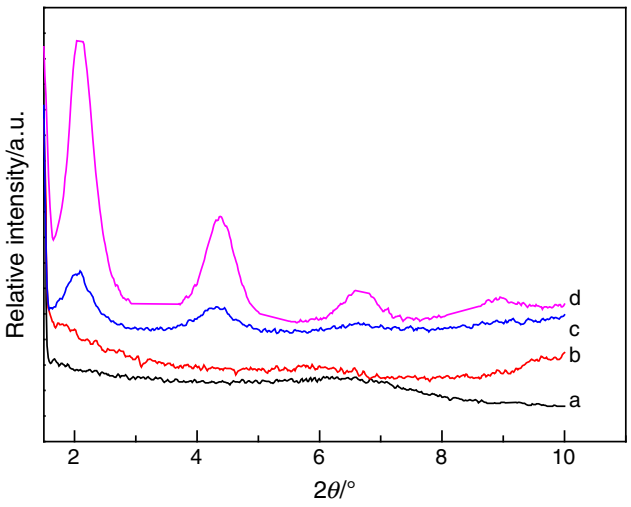

Fig. 1 XRD patterns of PP/IFR/Fe-OMT and comparative samples: *a* PP4 (2 %); *b* PP5 (4 %); *c* PP6 (6 %); *d* PP7 (4 % Na-OMT)

Thermal stability of PP/IFR/Fe-OMT nanocomposites

The thermal properties of PP/IFR, PP/IFR/Fe-OMT, and PP/IFR/Na-OMT composites were characterized by TG, as shown in Fig. 3. In the initial stage of thermal degradation (from 280 to 330 °C), the thermal properties of PP/IFR/Fe-OMT (Fig. 3b, d, e) and PP/IFR/Na-OMT (Fig. 3c) nanocomposites were not improved compared with that of PP/IFR (Fig. 3a) composites, which may be due to the decomposition of IFR. When the temperature was over 340 °C, the thermal stability of the PP/IFR/clay nanocomposites is noticeably improved by the addition of clay to the PP matrix. In Fig. 3c and d (PP5 and PP7), when the content of OMT was 4 %, the thermal stability of PP/IFR/Fe-OMT nanocomposites was higher than that of PP/IFR/Na-OMT nanocomposites, which indicated that the effect on thermal properties of Fe-OMT in PP/IFR matrix was superior to that of Na-OMT. The char residue of PP5 was higher than that of PP7 in 600 °C. It can be concluded that Fe-OMT was superior to Na-OMT in enhancing the temperature of the charring in PP/IFR system and the amount of charring for PP/IFR/Fe-OMT nanocomposites was higher than that for PP/IFR/Na-OMT nanocomposites. It indicated that the synergistic effect between Fe-OMT and PP/IFR is superior to that of Na-OMT and PP/IFR. It is believed that the presence of iron does lead some radical trapping, which enhances the thermal stability and charring ratio [19, 20].

Combustion performance of PP/IFR/Fe-OMT nanocomposites

The results of burning properties for PP, PP/IFR, PP/IFR/Fe-OMT, and PP/IFR/Na-OMT nanocomposites were shown in Table 2. The LOI and the UL-94 vertical burning test of PP indicate that flammability properties of nanocomposites are improved significantly compared with PP. The LOIs of PP5 (4 % Fe-OMT) and PP7 (4 % Na-OMT) are 26 and 24, respectively. It is notable that the dripping

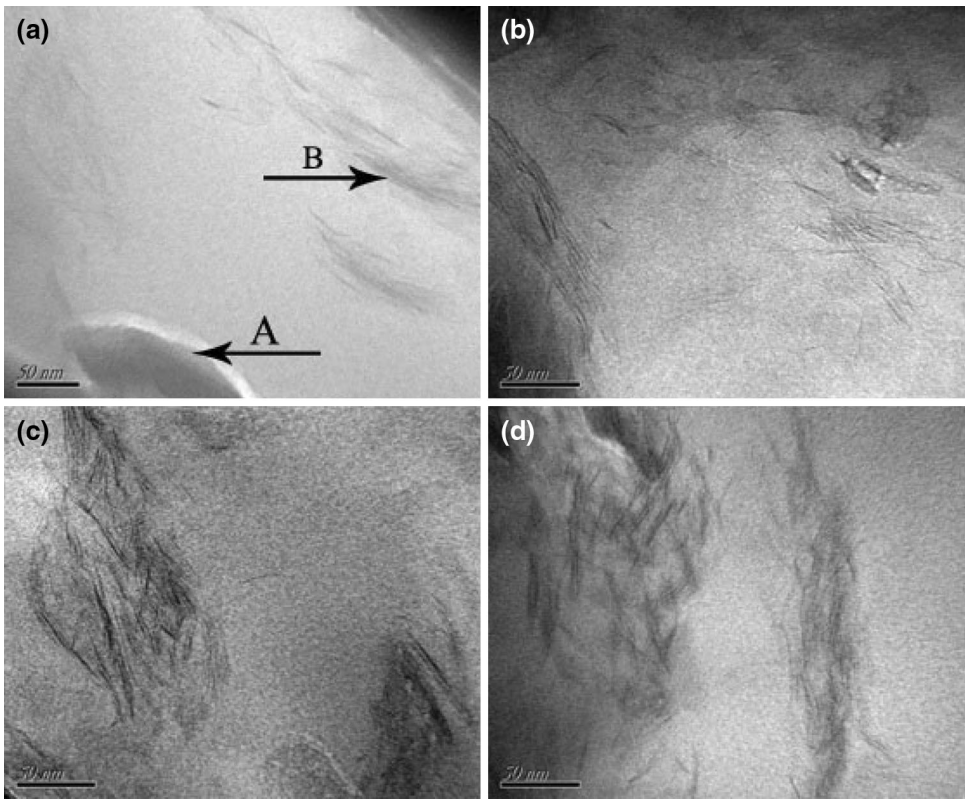

Fig. 2 TEM images of the nanocomposites: **a** PP4; **b** PP5; **c** PP6; **d** PP7

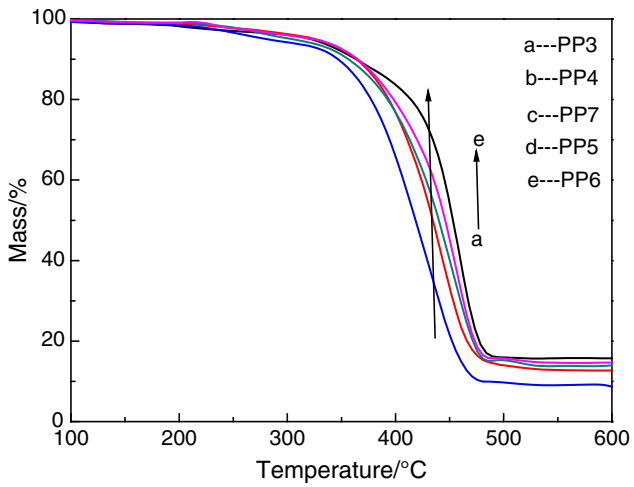

Fig. 3 TG curves in N_2 flow: *a* PP3; *b* PP4; *c* PP7; *d* PP5; *e* PP6

Table 2 The results of LOI, UL94, and MSD of composites

Samples	LOI	UL94	MSD
PP0	17	Burning, drippy	93.4
PP1	21	Burning, drippy	90.5
PP2	24	V-2	48.3
PP3	23	Burning, drippy	81.7
PP4	25	V-2	26.7
PP5	26	V-1	12.6
PP6	29	V-0	8.7
PP7	24	Burning, drippy	65.2
PP8	26	V-1	73.9
PP9	30	V-0	6.4

phenomenon is eliminated in the PP/IFR/Fe-OMT nanocomposites, but PP/IFR/Na-OMT nanocomposites still have dripping phenomenon and the improvement of LOI is also less. When the content of Fe-OMT is increased to 6 %, UL-94 achieves a V-0 grade. The effect of Fe-OMT in flame retardancy of PP is superior to that of Na-OMT, which indicates that Fe-OMT has better synergistic effect on the flame retardancy of PP/IFR composites. The similar results were also reported that the transition metal compounds were good synergistic agents in flame retardancy of polymer [21–23]. For example nickel formate was used as catalyst to improve the flame retardancy of intumescent systems in EVA systems [15].

The smoke density of PP/IFR/Fe-OMT nanocomposites

The results of the SDT are displayed in Table 2 and Fig. 4. MSD is the percent transmittance at maximum smoke density. The MSD of all the samples was shown in Table 2. From the results, the MSDs of PP/Fe-OMT nanocomposites were descended obviously comparing with the samples

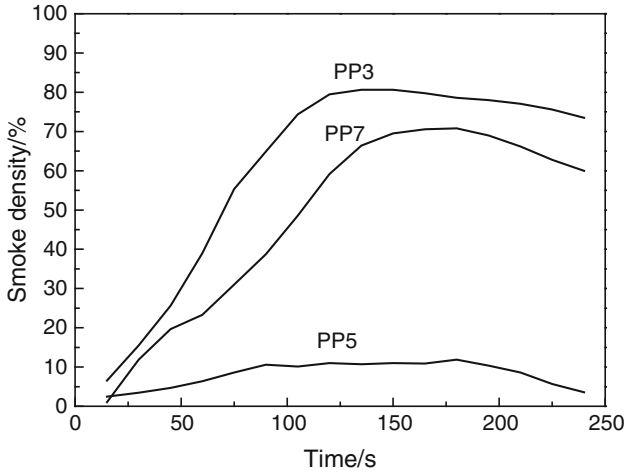

Fig. 4 Smoke density of PP3, PP5, PP7

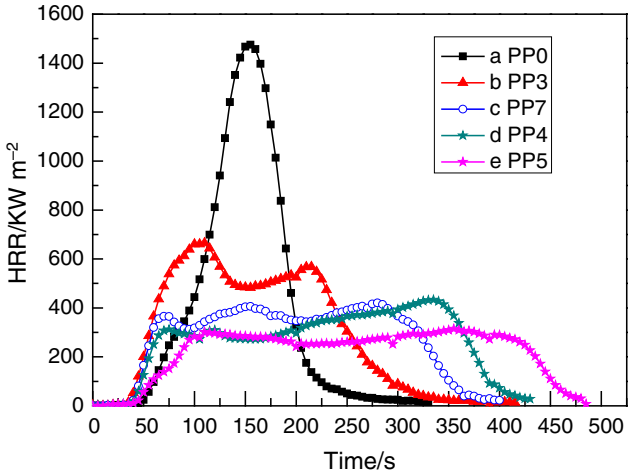

Fig. 5 The PP/IFR/Fe-OMT nanocomposites curves of HRR

that were free of Fe-OMT. In the Fig. 4, there were the results of smoke density PP3, PP5, and PP7. The smoke density of PP5 was lower than that of PP3 and PP7, and the smoke density of PP5 is about 1/8 of PP3 and 1/6 of PP7. The results revealed that Fe-OMT can reduce the production of smoke and the effect of Fe-OMT is superior to that of Na-OMT in the PP/IFR system. About the good synergistic flame retardant between Fe-OMT and PP/IFR, Fe ions may be the major effect in the PP/IFR/Fe-OMT nanocomposites. The mechanism of smoke suppression may be that the presence of iron does enhance the charring ratio [19, 24, 25].

Cone calorimeter test of PP/IFR/Fe-OMT nanocomposites

CCT results can be used to predict the combustion behavior of materials in a real fire [26]. And the CCT provides a wealth of information on the combustion behavior [2]. The measured heat release rate (HRR) curves of each sample were shown in Fig. 5. It can be seen that the pure PP burns faster after ignition and a sharp peak heat release rate (PHRR) appears with a PHRR value of 1,486.3 kW m^{-2}. In the case of PP3, PP4, PP5, and PP7, the PHRR values are greatly reduced, and the combustion times of the composites are prolonged in comparison with that of pure PP. When the amounts of Fe-OMT are 2 and 4 %, the PHRRs of PP4 and PP5 are 412.6 and 329.2 kW m^{-2}, respectively. The results reveal that PHRRs of PP/IFR/Fe-OMT nanocomposites are reduced with increasing the content of Fe-OMT. When 4 % Na-OMT is used as synergistic agent, the PHRR is 424.3 kW m^{-2}, so it can be believed that the flame-resistant effect of Fe-OMT is superior to that of Na-OMT on HRR. The suggested

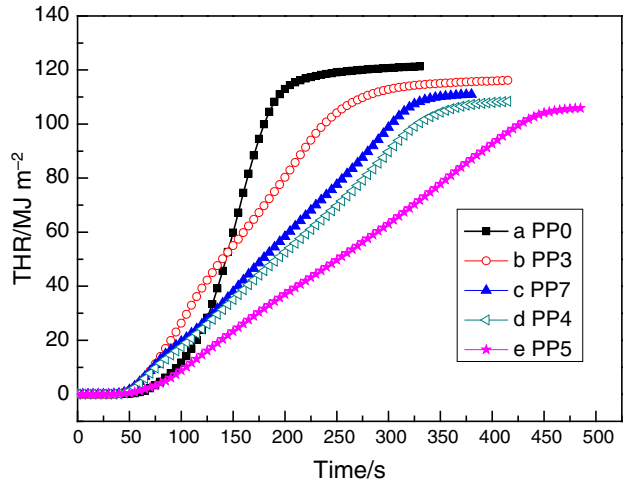

Fig. 6 The PP/IFR/Fe-OMT nanocomposites curves of THR

mechanism may be that the char layer serves as a barrier to both mass and energy transport by the functionalization of Fe-OMT.

Figure 6 presents the total heat release (THR) of all samples. It can be seen that the THR value of sample PP0 without any fire retardant is the highest among all samples. It is reported that the gradient of THR curve can be assumed as representative of flame spread [27]. Compared with sample PP0, the gradient of THR curve from sample PP3 with only IFR has some reduction, indicating the flame spread speed slows down. When Fe-OMT and Na-OMT are incorporated into the intumescent fire retardant coatings system, the THR values further decrease compared with sample PP3 which only IFR is added. Furthermore, comparing with the THR values of PP7 and PP5, the effect of

Fe-OMT on flame spread speed is superior to that of Na-OMT. The reason is that there is much compact char residue formed on the surface of the sample, restricting flame spreading. Among all the samples, sample PP4 and PP5 with IFR and Fe-OMT displays the smallest THR value, which is corresponded with the HRR curves in Fig. 5. It was reasonable that the amount of forming char becomes more with increasing the fraction of Fe-OMT, which makes THR decrease. The iron compounds in the polymer/IFR systems can improve the char formation [4]. The other reasons may be that Fe-MMT has the presence of structural iron and the burning of polymer is the free radical chain reaction, so structural iron is the operative site for radical trapping within the clay in the burning course of polymer nanocomposites.

Conclusions

PP/IFR/Fe-OMT nanocomposites were prepared by a melt-intercalation process. The corresponding PP/IFR/Na-OMT nanocomposites and PP/IFR composites were prepared under the same conditions. The results of XRD and TEM indicate that the nanocomposites were exfoliated and intercalated structures. The thermal stability, flame retardancy, and smoke suppression performance of PP/IFR/Fe-OMT nanocomposites were better than those of PP, PP/IFR composites, and PP/IFR/Na-OMT nanocomposites, which indicated that Fe-OMT can produce effectively synergistic flame retardant influence with IFR in the PP system.

Acknowledgements The work was financially supported by the China Postdoctoral Science Foundation (No. 2012M511210), the research fund of Key Laboratory for Advanced Technology in Environmental Protection of Jiangsu Province (No. AE201104), Natural Science Foundation of the Higher Education Institutions of Jiangsu Province (No. 13KJB430012), the Opening Project of CAS Key Laboratory of Materials for Energy Conversion, and Jiangsu Province College Students' Innovative Projects (201310299026).

References

1. Ewen JA, Elder MJ, Jones RL, Rheingold AL, Liable-Sands LM, Sommer RD. Chiral ansa metallocenes with Cp ring-fused to thiophenes and pyrroles: syntheses, crystal structures, and isotactic polypropylene catalysts. J Am Chem Soc. 2001;123:4763–73.
2. Liu Y, Zhao J, Deng CL, Chen L, Wang DY, Wang YZ. Flame-retardant effect of sepiolite on an intumescent flame-retardant polypropylene system. Ind Eng Chem Res. 2011;50:2047–54.
3. Wang XY, Li Y, Liao WW, Gu J, Li D. A new intumescent flame-retardant: preparation, surface modification, and its application in polypropylene. Polym Adv Technol. 2008;19:1055–61.
4. Wang L, Yang W, Wang BB, Wu Y, Hu Y, Song L, Yuen RK. The Impact of metal oxides on the combustion behavior of ethylene–vinyl acetate copolymers containing an intumescent flame retardant. Ind Eng Chem Res. 2012;51:7884–90.
5. Huang GB, Yang JG, Wang X, Gao JR. Nanoclay, intumescent flame retardants, and their combination with chemical modification for the improvement of the flame retardant properties of polymer nanocomposites. Polym Int. 2013;21:27–34.
6. Nie SB, Zhang MX, Yuan SJ, Dai GL, Hong NN, Song L, Hu Y, Liu XL. Thermal and flame retardant properties of novel intumescent flame retardant low-density polyethylene (LDPE) composites. J Therm Anal Calorim. 2012;109:999–1004.
7. Xie F, Wang YZ, Yang B, Liu Y. A novel intumescent flame-retardant polyethylene system. Macromol Mater Eng. 2006;291:247–53.
8. Liang JZ. Tensile properties of polypropylene flame-retardant composites. Polym Bull. 2012;68:803–13.
9. Camino G, Grassie N, McNeill IC. Influence of the fire retardant, ammonium polyphosphate, on the thermal degradation of poly(-methyl methacrylate). J Polym Sci. 1978;1:95–106.
10. Li B, Sun CY, Zhang XC. An investigation of flammability of intumescent flame retardant polyethylene containing starch by using cone calorimeter. Chem J Chin Univ. 1999;20:146–9.
11. Shen ZQ, Chen L, Lin L, Deng CL, Zhao J, Wang YZ. Synergistic effect of layered nanofillers in intumescent flame-retardant EPDM: montmorillonite versus layered double hydroxides. Ind Eng Chem Res. 2013;52:8454–63.
12. Lin M, Li B, Li QF, Li S, Zhang SQ. Synergistic effect of metal oxides on the flame retardancy and thermal degradation of novel intumescent flame-retardant thermoplastic polyurethanes. J Appl Polym Sci. 2011;121:1951–60.
13. Wu N, Yang RJ. Effects of metal oxides on intumescent flame-retardant polypropylene. Polym Adv Technol. 2011;22:495–501.
14. Li YT, Li B, Dai JF, Jia H, Gao SL. Synergistic effects of lanthanum oxide on a novel intumescent flame retardant polypropylene system. Polym Degrad Stab. 2008;93:9–16.
15. Zhou KQ, Wang BB, Jiang SH, Yuan HX, Song L, Hu Y. Facile preparation of nickel phosphide ($Ni_{12}P_5$) and synergistic effect with intumescent flame retardants in ethylene–vinyl acetate copolymer. Ind Eng Chem Res. 2013;52:6303–10.
16. Chen XC, Ding YP, Tang T. Synergistic effect of nickel formate on the thermal and flame-retardant properties of polypropylene. Polym Int. 2005;54:904–8.
17. Tian NN, Wen X, Jiang ZW, Gong J, Wang YH, Xue J, Tang T. Synergistic effect between a novel char forming agent and ammonium polyphosphate on flame retardancy and thermal properties of polypropylene. Ind Eng Chem Res. 2013;52:10905–15.
18. Sun LS, Qu YT, Li SX. Co-microencapsulate of ammonium polyphosphate and pentaerythritol in intumescent flame-retardant coatings. J Therm Anal Calorim. 2013;111:1099–106.
19. Kong QH, Tang YW, Hu Y, Song L, Liu H, Li LX. Thermal stability and flame retardance properties, of acrylonitrile-butadiene-styrene/polyvinyl chloride/organophilic Fe-montmorillonite nanocomposites. J Polym Res. 2012;19:9751–60.
20. Zhu J, Uhl FM, Morgan AB, Wilkie CA. Studies on the mechanism by which the formation of nanocomposites enhances thermal stability. Chem Mater. 2001;13:4649–54.
21. Gallo E, Schartel B, Braun U, Russo P, Acierno D. Fire retardant synergisms between nanometric Fe_2O_3 and aluminum phosphinate in poly(butylene terephthalate). Polym Adv Technol. 2011;22:2382–91.
22. Lewin M, Endo M. Catalysis of intumescent flame retardancy of polypropylene by metallic compounds. Polym Adv Technol. 2003;14:3–11.

23. Song RJ, Jiang ZW, Yu HO, Liu J, Zhang ZJ, Wang QW, Tang T. Strengthening carbon deposition of polyolefin using combined catalyst as a general method for improving fire retardancy. Macromol Rapid Commun. 2008;29:789–93.
24. Wu WH, Xie JX, Xu JZ, Qu HQ. Zinc hydroxystannate-coated metal hydroxides as flame retardant and smoke suppression for flexible poly vinyl chloride. Fire Mater. 2009;33:201–10.
25. Carty P. Flame retardants: iron compounds, their effect on fire and smoke in halogenated polymers. In: Pritchard G, editor. Plastics Additives., Polymer Science and Technology SeriesD-ordrecht: Springer; 1998. p. 307–14.
26. Kuzawa K, Jung YJ, Kiso Y, Yamada T, Nagai M, Lee TG. Phosphate removal and recovery with a synthetic hydrotalcite as an adsorbent. Chemosphere. 2006;62:45–52.
27. Jiao CM, Chen XL. Flammability and thermal degradation of intumescent flame-retardant polypropylene composites. Polym Eng Sci. 2010;10:767–72.